NEOPLASIA
www.neoplasia.com

Volume 12 Number 2 February 2010 pp. 116–127 116

GAS6/AXL Axis Regulates Prostate Cancer Invasion, Proliferation, and Survival in the Bone Marrow Niche[1,2]

Yusuke Shiozawa*, Elisabeth A. Pedersen*, Lalit R. Patel†, Anne M. Ziegler*, Aaron M. Havens*,‡, Younghun Jung*, Jingcheng Wang*, Stephanie Zalucha*, Robert D. Loberg†, Kenneth J. Pienta† and Russell S. Taichman*

*Department of Periodontics and Oral Medicine, University of Michigan School of Dentistry, Ann Arbor, MI, USA; †Departments of Urology and Internal Medicine, University of Michigan School of Medicine, Ann Arbor, MI, USA; ‡Harvard School of Dental Medicine, Boston, MA, USA

Abstract

Our recent studies have shown that annexin II, expressed on the cell surface of osteoblasts, plays an important role in the adhesion of hematopoietic stem cells (HSCs) to the endosteal niche. Similarly, prostate cancer (PCa) cells express the annexin II receptor and seem to use the stem cell niche for homing to the bone marrow. The role of the niche is thought to be the induction and sustenance of HSC dormancy. If metastatic PCa cells occupy a similar or the same ecological niche as HSCs, then it is likely that the initial role of the HSC niche will be to induce dormancy in metastatic cells. In this study, we demonstrate that the binding of PCa to annexin II induces the expression of the growth arrest–specific 6 (GAS6) receptors AXL, Sky, and Mer, which, in the hematopoietic system, induce dormancy. In addition, GAS6 produced by osteoblasts prevents PCa proliferation and protects PCa from chemotherapy-induced apoptosis. Our results suggest that the activation of GAS6 receptors on PCa in the bone marrow environment may play a critical role as a molecular switch, establishing metastatic tumor cell dormancy.

Neoplasia (2010) 12, 116–127

Introduction

Nearly 10% of patients whose conditions are diagnosed as PCa initially present with bone metastasis and almost all patients who die of prostate cancers (PCas) have skeletal involvement [1]. Therefore, identifying the mechanisms that control bone metastasis is of great consequence to facilitate the design of therapeutics aimed at decreasing metastatic risk and/or their complications.

The metastatic process is similar to "homing" behavior of hematopoietic stem cells (HSCs) to the bone marrow. In marrow, HSCs reside in an area that is defined as the stem cell "niche." Identification of the HSC niche in marrow has been an active area of investigation. Works in this field have demonstrated that several molecules expressed by osteoblasts [2–6] and endothelial cells [7] play critical roles in niche selection. Recently, it was shown that 1) the engraftment of HSCs in lethally irradiated animals during experimental bone marrow transplantation and 2) PCa metastasis to the marrow are dependent on many of the same molecules [8,9].

Several studies have shown that disseminated cells shed from a primary tumor may lie dormant in distant tissues for long periods before they can be activated to form metastases [10–12]. At present, there is little information on how dormancy is induced or what leads to the activation of the dormant cells. One hypothesis worth considering is that molecules that induce HSC dormancy are likely to induce dormancy of metastatic PCa cells. Where adhesion molecules and secreted factors derived from the HSC niche are thought to regulate HSC self-renewal, proliferation, and differentiation [13].

Address all correspondence to: Russell S. Taichman, DMD, DMSc, Department of Periodontics and Oral Medicine, University of Michigan School of Dentistry, Room 3307, 1011 North University Ave, Ann Arbor, MI 48109-1078. E-mail: rtaich@umich.edu

[1]This work is directly supported by the Charles Eliot Ware Memorial Fellowship (A.M.H.), the Pediatric Oncology Research Fellowship (Y.S.), the National Cancer Institute (K.J.P. and R.S.T.), the Department of Defense (K.J.P. and R.S.T.), and the Prostate Cancer Foundation (K.J.P. and R.S.T.). K.J.P. receives support as an American Cancer Society Clinical Research Professor.

[2]This article refers to supplementary material, which is designated by Figure W1 and is available online at www.neoplasia.com.

Received 15 August 2009; Revised 5 November 2009; Accepted 11 November 2009

DOI 10.1593/neo.91384

One protein in high abundance in the marrow is annexin II (Anxa2) [14]. Our recent work has shown that Anxa2 expressed by osteoblasts and endothelial cells plays a critical role in HSC niche selection [15]. More recently, we found that Anxa2 and the Anxa2 receptor (Anxa2r) axis plays a crucial role in establishing bone metastases of PCa [9] by regulating PCa migration, adhesion, and growth in the bone marrow [9]. Blocking Anxa2 or Anxa2r limited short-term and long-term localization of human PCa in murine models, further demonstrating the role of this axis [9].

To further explore the role that Anxa2 plays in the interactions of both PCa and HSCs and the endosteal niche, we added purified Anxa2 protein to PCa cells *in vitro*. Gene expression microarray analysis demonstrated that expression of the receptor tyrosine kinase (RTK) AXL (from the Greek word *anexelekto* or uncontrolled) was enhance in PCa after exposure to Anxa2 (unpublished observations). AXL binds to and is activated by the growth factor growth arrest–specific 6 (GAS6) [16]. In many systems, including HSCs, GAS6 inhibits cellular proliferation and enhances cell survival [17–22]. Intriguingly, GAS6 expressed by stromal cells slows the cell cycling of HSCs [21].

In the present report, it is demonstrated that the engagement of Anxa2rs on PCa stimulates the expression of AXL receptors. In contrast with previous reports, we found that GAS6 inhibits PCa proliferation, a situation more closely mimicking that of HSCs. These findings suggest that GAS6 may participate in the induction of tumor cell dormancy so that disseminated cells shed from a primary tumor may lie dormant for prolonged periods in marrow. These observations suggest further parallels between the regulation of HSC function in their endosteal niche and the formation of PCa bone metastases.

Materials and Methods

Cell Culture

PC3 (CRL-1435), DU145 (HTB-81), and LNCaP (CRL-1740) PCa cell lines were obtained from the American Type Culture Collection (Rockville, MD). The metastatic subline LNCaP C4-2B was originally isolated from a lymph node of a patient with disseminated bony and lymph node involvement [23]. SaOS2 (HTB-85) and MG63 (CRL-1427) osteosarcoma cell lines were also obtained from the American Type Culture Collection. PCa cell lines and osteosarcoma cell lines were cultured in RPMI 1640 (Invitrogen, Carlsbad, CA) and Dulbecco's modified Eagle medium (Invitrogen), respectively. All cultures were supplemented with 10% (vol./vol.) fetal bovine serum (FBS; Invitrogen) and 1% (vol./vol.) penicillin-streptomycin (Invitrogen) and maintained at 37°C, 5% CO_2, and 100% humidity.

Human Osteoblasts

Human osteoblasts were established by explant culture from normal human trabecular bone obtained from patients undergoing orthopedic surgery in accordance with the University of Michigan's Investigational Review Board, as previously described [3].

Antibodies and Reagents

The anti-AXL antibody (clone 108724; mouse immunoglobulin G subclass 1 [IgG1]) and the anti-Mer antibody (clone 125518; mouse IgG1) were purchased from R&D Systems (Minneapolis, MN). The anti-Anxa2 antibody (clone 5; mouse IgG1) was purchased from BD Pharmingen (San Diego, CA). Zenon Alexa Fluor 488 and 555 antibody labeling kits were purchased from Molecular Probes (Eugene, OR). The control antibodies for these investigations included IgG1 (clone X40; Becton Dickinson, San Jose, CA). The antibodies to phosphorylated p44/42 mitogen-activated protein (MAP) kinase (Thr202/Tyr204), total p44/42 MAP kinase, and horseradish peroxidase–labeled goat anti-rabbit IgG (H + L) were obtained from Cell Signaling Technology (Danvers, MA). Anxa2 N-terminal peptide corresponding to the 1 to 12 amino acids and a random peptide (TVLLHEICKSSL) were synthesized, as previously detailed [15]. Recombinant human GAS6 was kindly provided by Amgen (Thousand Oaks, CA).

Anxa2 Treatments

PCa cell lines (1×10^6 cells/well) were cultured in six-well plates in RPMI medium (1 ml) without FBS for 5 hours. After serum starvation, the cells were treated with 1 μg/ml of Anxa2 N-terminal peptide for 24 hours. The cells were analyzed for messenger RNA (mRNA) of AXL, Sky, and Mer by real-time quantitative reverse transcription–polymerase chain reaction (QRT-PCR). In some cases, PC3 cells were analyzed for surface expression of AXL and Mer by flow cytometry.

RNA Extraction and QRT-PCR

QRT-PCR was carried out using standard techniques. Briefly, total RNA was isolated using RNeasy Mini Kit (Qiagen, Valencia, CA), and first-strand complementary DNA was synthesized in a 20-μl reaction volume using 0.4 μg of total RNA. Reverse transcript products were analyzed by QRT-PCR in TaqMan Gene Expression Assays of several target genes including GAS6, AXL, Sky, Mer, and β-Actin (Applied Biosystems, Foster City, CA). QRT-PCR analysis was performed using 15.0 μl of TaqMan Universal PCR Master Mix (Applied Biosystems), 1.5 μl of TaqMan Gene Expression Assay, 1 μl of complementary DNA, and RNAse/DNAse–free water in a total volume of 30 μl. All sample concentrations were standardized in each reaction to exclude false-positive results. Reactions without template and/or enzyme were used as negative controls. The second-step PCR (95°C for 30 seconds and 60°C for 1 minute) was run for 40 cycles after an initial single cycle of 95°C for 15 minutes to activate the Taq polymerase. The PCR product was detected as an increase in fluorescence using an ABI PRISM 7700 sequence detection system (Applied Biosystems). RNA quantity (C_R) was normalized to the housekeeping gene *β-actin* control by using the formula $C_R = 2^{(40 - Ct \text{ of sample}) - (40 - Ct \text{ of control})}$. The threshold cycle ($C_t$) is the cycle at which a significant increase in fluorescence occurs.

Flow Cytometry

PC3 cells were stained with anti-AXL or anti-Mer antibody or isotype-matched IgG control. Flow cytometric analyses were performed in a FACS Vantage dual-laser flow cytometer (Becton Dickinson).

Western Blot Analyses

PC3 cells (1×10^6 cells/well) were cultured in six-well plates in RPMI medium (1 ml) without FBS for 5 hours. After serum starvation, the cells were treated with 1 μg/ml GAS6 for 5, 15, 30, 45, and 60 minutes. In some cases, PC3 cells or SaOS2 cells were treated with 1 μg/ml GAS6 and/or 1 μg/ml Anxa2 for 60 minutes. The cells were extracted for protein and analyzed for phosphorylated p44/42 MAP kinase (Thr202/Tyr204) by Western blot analysis. Total p44/42 MAP kinase was used as an internal control for loading.

Tissue Microarray and Immunostaining

Human prostate adenocarcinoma tissue microarray was purchased from US Biomax (Rockville, MD). Tumors were graded using the Gleason grading system and examined to identify areas of benign prostate, PCa, and bone metastasis. The formalin-fixed, paraffin-embedded tissues were deparaffinized and placed in a pressure cooker containing 0.01 M buffered sodium citrate solution (pH 6.0), boiled, and chilled to room temperature for antigen retrieval. The slides were incubated overnight at room temperature with anti-AXL antibody diluted 1:100. In some cases, the slides were costained with anti-AXL antibody (prestained with Zenon Alexa Fluor 555) and anti-Anxa2 antibody (prestained with Zenon Alexa Fluor 488). A pathologist blinded to the study analyzed the arrays, and staining intensity was ranked on a scale from 0 to 3 (0, negative; 1, weak; 2, moderate; and 3, strong intensity staining).

Vertebral Body Transplants (Vossicles)

Vertebral body transplantations were performed, as previously described [9]. Lumbar vertebrae were isolated from *Anxa2*$^{+/+}$ or *Anxa2*$^{-/-}$ mice 7 days after birth. The vertebrae were sectioned into single vertebral bodies (vossicles). Athymic (nude) mice were used as transplant recipients. Four vossicles were implanted per mouse into subcutaneous pouches. Before implantation, PC3 cells were introduced into both *Anxa2*$^{+/+}$ and *Anxa2*$^{-/-}$ vossicles by injection of 1×10^4 cells in 10 μl of PBS. At 30 days after implantation, vossicles were collected and stained with anti-AXL antibody or isotype-matched IgG control.

GAS6 ELISA

Antibody sandwich ELISAs were used to measure GAS6 secreted by human osteoblasts and osteosarcoma cell lines SaOS2 and MG63 (4×10^4 cells) into serum-free cell culture medium (R&D Systems). In some cases, after 24 hours of serum starvation, PC3 cells in 100 μl of RPMI 1640 supplemented without FBS were overlaid at 0 to 4×10^4 cells per well onto the osteoblasts directly. GAS6 levels were normalized to total protein in the cell culture–conditioned medium.

Transwell Invasion Assays

Cell invasion into a reconstituted extracellular matrix coating of Matrigel laid over polyethylene terephthalate membranes with an 8-μm pore size was performed in dual-chambered invasion plates (BD Biosciences, San Jose, CA) as previously described [24,25]. Assayed cells were placed in the upper chamber (1×10^5 cells/well) in serum-free RPMI. Spontaneous invasion was compared with invasion supported by GAS6 (0-1 μg/ml). At termination of the assay (24 hours), chambers were removed, 40 μl of 3-(4,5-dimethylthiazol-2-yl)-2,5-diphenyltetrazolium bromide (MTT; 5 mg/ml; Sigma-Aldrich, St. Louis, MO) was added to the top well, and 80 μl of MTT was added to the bottom wells before incubation for an additional 4 hours at 37°C. After completely removing residual medium or cells from the top chamber, the purple residues were released from the bottom of the invasion chambers, inside the invasion matrix, and from the bottom of the upper chamber with 1 ml of isopropanol (Sigma-Aldrich). The invasion chambers were rocked for 30 minutes at a medium speed before reading 100 μl from each well on a multiwell scanning spectrophotometer (Molecular Devices, Sunnyvale, CA) at OD_{450}.

Proliferation Assays

PC3 cells were plated into triplicate 96-well plates at a concentration of 5000 cells per well (100 μl per well) in growth medium with 0.1% FBS. After 24 hours, cells were treated with serial doses of rhGAS6 (0-1 μg/ml). In some cases, proliferation of PC3 cells in response of GAS6 and/or Anxa2 was examined with/without 10 μM of U0126 for 1 hour (MAPK kinase [MEK] 1/2 inhibitor; Cell Signaling Technology). Thereafter, the cultures were incubated in an atmosphere of 5% CO_2 and 95% O_2 at 37°C for 3 days. Proliferation was quantified using sodium 3′-[1-[(phenylamino)-carbonyl]-3,4-tetrazolium]-bis(4-methoxy-6-nitro)benzene-sulfonic acid hydrate (XTT) colorimetric assay (Sigma-Aldrich). Optical intensities were read on a multiwell scanning spectrophotometer at OD_{492} (Molecular Devices).

Apoptosis Assays

PC3 cells (1×10^6 cells/well) were cultured in six-well plates in RPMI medium (1 ml) without FBS for 5 hours. After serum starvation, the cells were treated with 1 μg/ml of GAS6 for 24 hours. In certain cases, PC3 cells (1×10^5 cells/well) were cultured in six-well plates in RPMI medium (1 ml) with 5% FBS for 5 hours. Thereafter, the cells were treated with 1 μg/ml GAS6 for 24 hours. In some cases, PC3 cells were treated with 1 μg/ml of Anxa2 peptide for 24 hours before GAS6 treatment. After 24 hours of incubation, the cells were treated with Taxotere (0.4 μg/ml) for 48 hours. Cells were stained for apoptosis using annexin V PE (BD Biosciences) and 7AAD (BD Biosciences), according to the manufacturer's protocol. Apoptotic cells were quantified by flow cytometry.

Cell Cycling Assays

Cell cycle status of PC3 cells treated with Anxa2 and/or GAS6 were analyzed by FACS using Hoechst 33342 (Molecular Probes) and Pyronin Y (PY; Sigma-Aldrich) staining methods, as previously described [26]. Briefly, PC3 cells (1×10^6 cells per well) were cultured in six-well plates in RPMI medium (1 ml) without FBS for 5 hours and were treated with 1 μg/ml of GAS6 or vehicle for 48 hours. In some cases, PC3 cells were treated with 1 μg/ml of Anxa2 peptide for 24 hours before GAS6 treatment. Thereafter, cells were incubated in 2 μg/ml of Hoechst 33342 for 45 minutes and were incubated in 4 μg/ml of PY for another 45 minutes. The cell cycle state was analyzed by flow cytometry. The cells that expressed low Hoechst 33342 and low PY, low Hoechst 33342 and high PY, and high Hoechst 33342 and high PY were determined as G_0, G_1, and $S/G_2/M$ states, respectively.

Quantification of Immunohistochemical Stains and Western Blots

The staining intensities of immunohistochemistry slides and the densities of the Western blot bands were quantified with ImageJ software (version 1.40; National Institutes of Health, Bethesda, MD).

Statistical Analyses

All *in vitro* experiments were performed at least three times with simi lar results. Results from representative assays are shown. Numerical data are expressed as mean ± SD. Statistical analysis was performed by analysis of variance or Student's *t* test using the GraphPad Instat statistical program (GraphPad Software, San Diego, CA) with significance at $P < .05$. For the QRT-PCR assays, a Kruskal-Wallis test and Dunn's multiple comparisons tests were used with the level of significance set at $P < .05$.

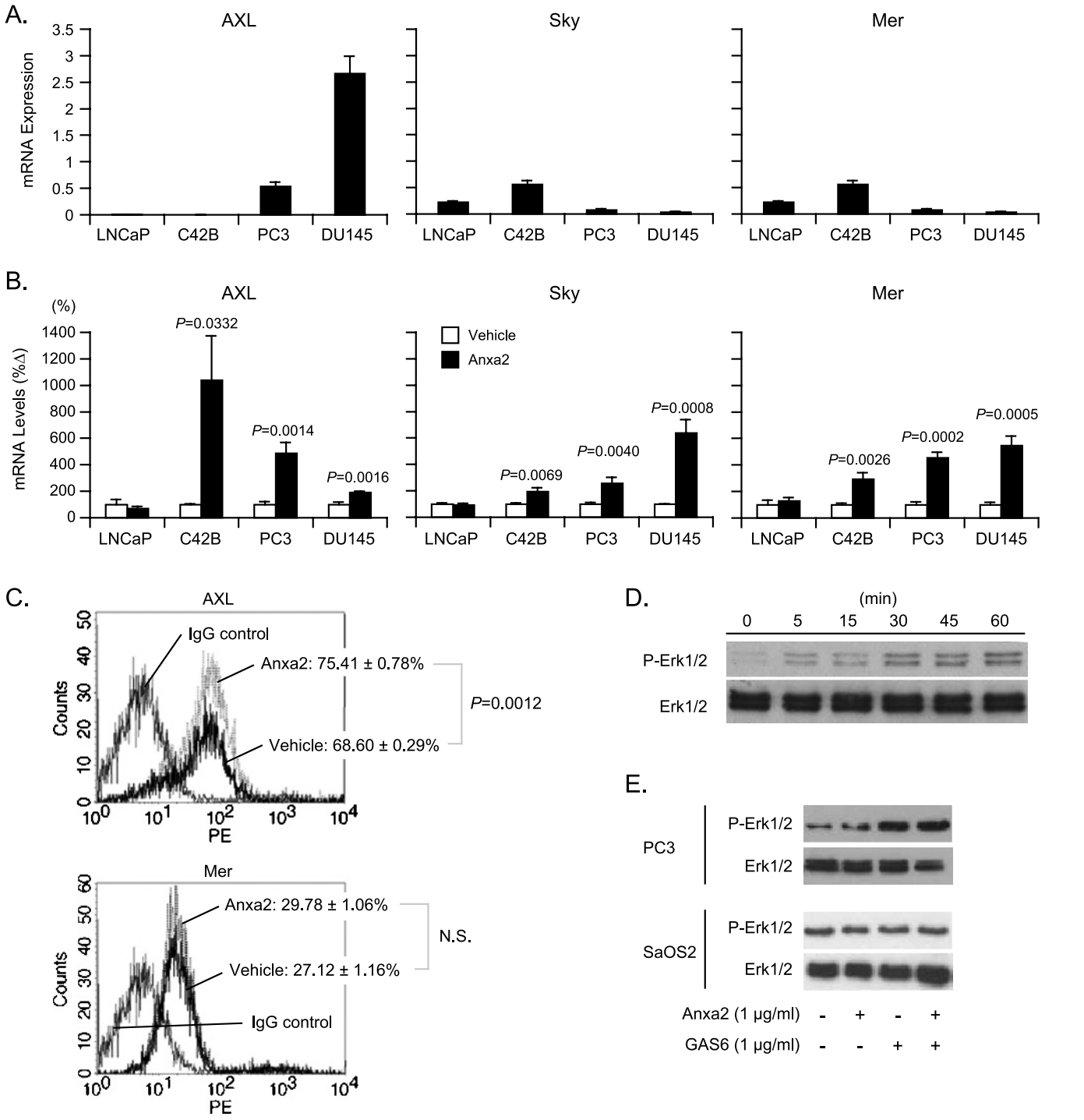

Figure 1. Anxa2-induced AXL family in PCa. (A) AXL, Sky, and Mer mRNA levels of PCa cell lines (LNCaP, C4-2B, PC3, and DU145) were determined by real time RT-PCR. Data were normalized to β-actin and are presented as mean ± SD from three independent PCRs. (B) PCa cell lines (LNCaP, C4-2B, PC3, and DU145) were treated with 1 μg/ml of N-terminal Anxa2 peptide for 24 hours, and RNA was isolated. The levels of mRNA were determined by real-time RT-PCR. Data were normalized to β-actin and presented as the mean ± SD from three independent PCRs. *Significant difference from vehicle treatment. (C) Representative flow cytometric analyses of AXL and Mer expression on PC3. PC3 cells were treated with 1 μg/ml of an N-terminal Anxa2 peptide for 24 hours. The expression levels of AXL and Mer were determined by flow cytometry. Data are presented as mean ± SD from triplicate determinations. Data are presented as the mean ± SD from three independent experiments. *Significant difference from vehicle treatment. *NS* indicates not significant. (D) PC3 cells were cultured in medium without FBS for 5 hours. After serum starvation, the cells were treated with 1 μg/ml of GAS6 for 5, 15, 30, 45, and 60 minutes. Total protein was extracted and analyzed by Western blot for phosphorylated Erk1/2. Total Erk1/2 was used as an internal control for loading. (E) PC3 cells and SaOS2 cells were cultured in medium without FBS for 5 hours. After serum starvation, the cells were treated with 1 μg/ml of Anxa2 and/or 1 μg/ml of GAS6 for 60 minutes. Total protein was extracted and analyzed by Western blot for phosphorylated Erk1/2. Total Erk1/2 was used as an internal control for loading.

Results

Anxa2 Stimulates PCa Expression of the AXL Subfamily of Tyrosine Kinase Receptors

Previously, we determined that Anxa2 expressed by osteoblasts plays a central role in niche selection by HSCs and in PCa metastasis [9,15]. To explore the interaction of Anxa2 and the AXL family of RTKs (AXL, Sky, and Mer), we first examined the basal expression levels of the AXL family of RTKs in PCa cell lines by QRT-PCR. High-level AXL expression was observed in DU145 and PC3 cells, whereas a low level of AXL expression was detected in LNCaP and C4-2B cells (Figure 1*A*). In comparison, higher Sky and Mer expression

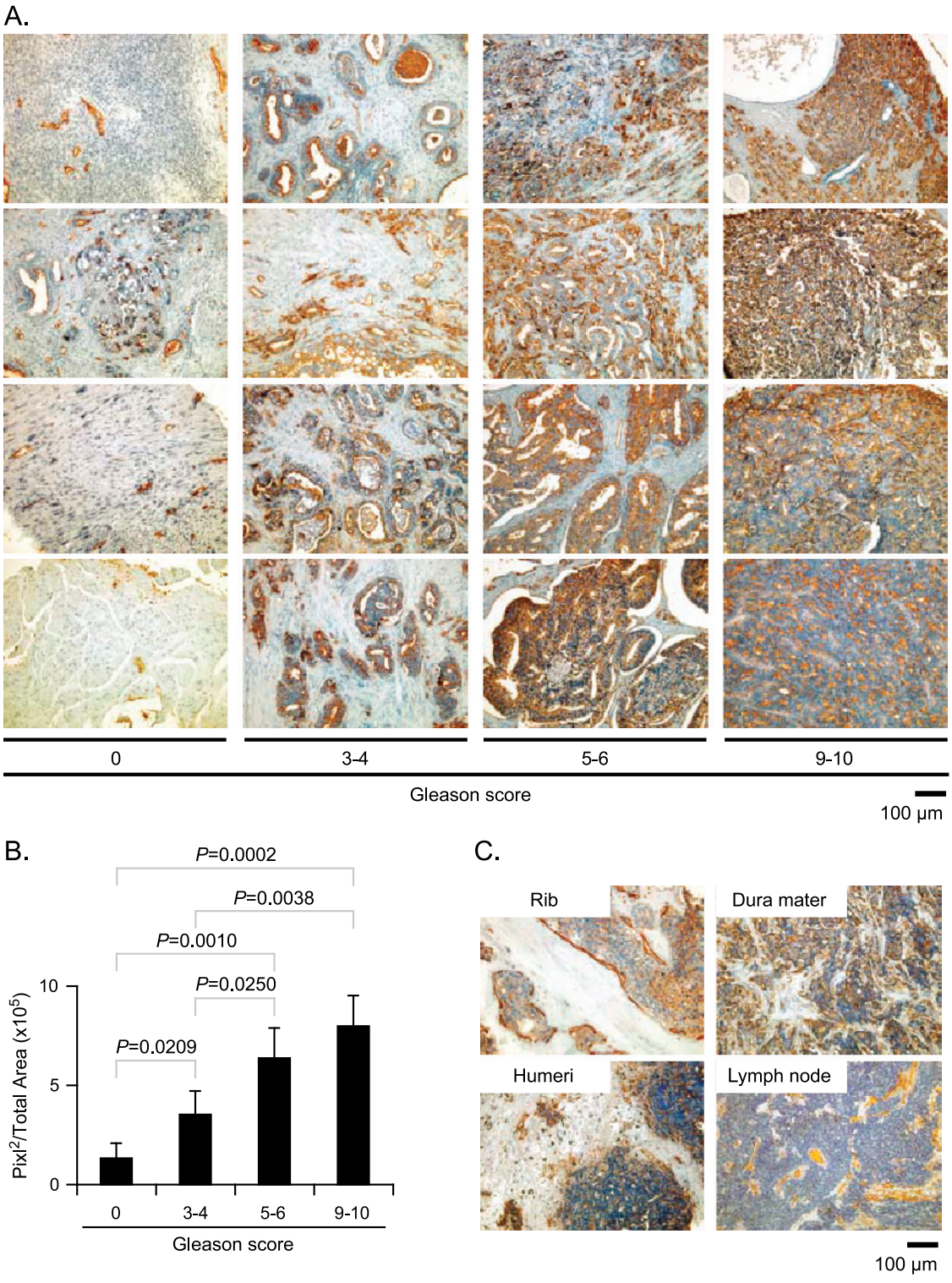

Figure 2. PCa expresses AXL. (A) Representative elements of a tissue microarray in PCa stained with anti-AXL antibodies. IgG staining control not shown. (B) Quantitative analysis of data presented in (A). (C) Representative elements of a tissue microarray in metastatic PCa stained with anti-AXL antibody. Original magnification, ×20. Scale bar, 100 μm.

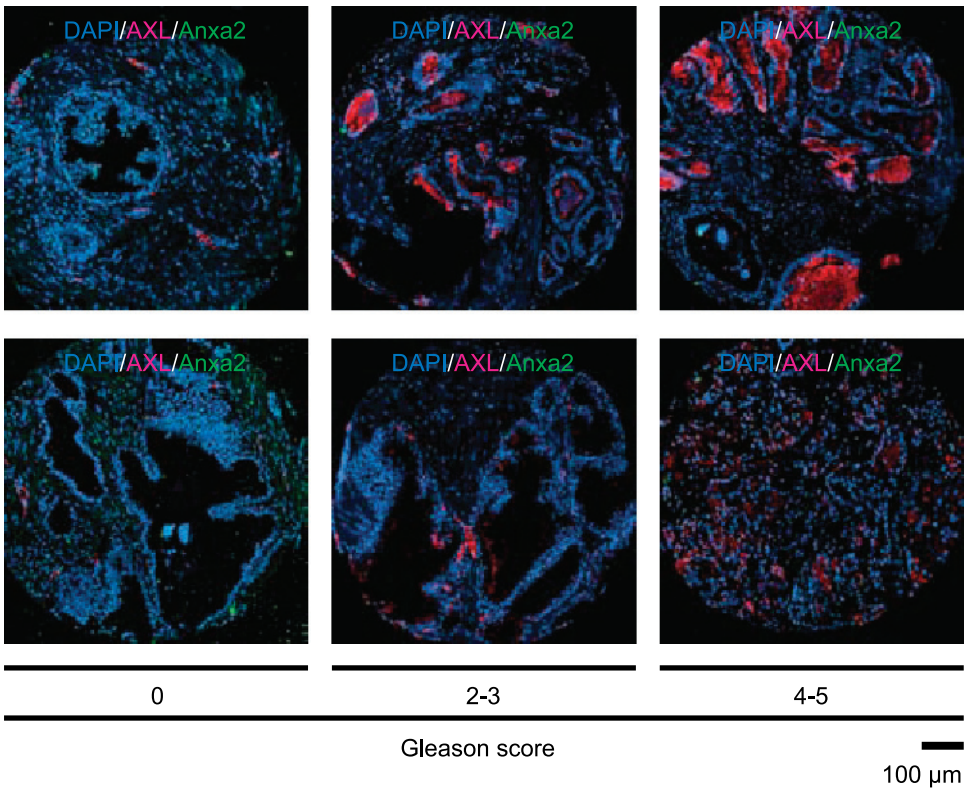

Figure 3. Interaction between the expression of AXL and Anxa2 in PCa. Representative elements of a tissue microarray in PCa costained with anti-AXL antibodies and anti-Anxa2 antibodies. Nuclei were identified by 4′,6-diamidino-2-phenylindole. Original magnification, ×20. Scale bar, 100 μm.

was detected in LNCaP and C4-2B cells than PC3 and DU145 cells (Figure 1*A*).

Next, we expanded our studies to examine mRNA levels of AXL and the other members of the AXL family of RTKs by PCa cell lines after stimulation with Anxa2. Interestingly, mRNA expression of each AXL family member was dramatically increased in DU145, PC3, and C4-2B, but not LNCaP cells at 24 hours after Anxa2 stimulation (Figure 1*B*). Flow cytometry was used to determine whether the changes in mRNA levels correspond with alterations in cell surface expression of AXL family RTKs. For these studies, PC3 cells were chosen because they expressed high basal levels of the AXL mRNA and responded robustly to Anxa2 stimulation (Figure 1, *A* and *B*). PC3 cells were treated with Anxa2 for 24 hours, and cell surface receptor expression was evaluated. As shown in Figure 1*C*, cell surface expression of AXL and Mer were easily distinguished from control IgG staining (a suitable antibody for Sky expression was not identified [data not presented]). More cell surface AXL expression was detected in Anxa2-treated cells than in vehicle-treated cells (75.4 ± 1.3% *vs* 68.6 ± 0.5%, $P = .0012$), whereas Mer expression was not altered (Figure 1*C*). To determine whether the expression of the AXL family of RTKs is activated in response to GAS6, an established ligand for all three Axl subfamily of RTKs [16] and PC3 cells was treated with GAS6. Phosphorylation of Erk1/2, a downstream effector of AXL signaling [16,27], after GAS6 treatment was evaluated by Western blot analysis. Data demonstrate that GAS6 rapidly induces Erk1/2 phosphorylation in PC3 cells within 5 minutes (Figures 1*D* and W1*A*). In addition, GAS6 and Anxa2 showed synergic effects on Erk1/2 phosphorylation (Figures 1*E* and W1*B*). However, no effects of Anxa2 and GAS6 on Erk1/2 phosphorylation in osteosarcoma cells were observed (Figures 1*E* and W1*C*). These findings suggest that GAS6 activates the AXL family of tyrosine kinase receptors in PCa cells.

The findings thus far suggest that AXL expression is regulated by Anxa2. Because Anxa2 is highly expressed in marrow, brain, and lymph nodes compared with other soft tissues [9,15], tissue microarrays were used to correlate AXL expression with metastasis. Tumors were graded using the Gleason grading system and examined to identify areas of benign prostate and PCa. Staining of microarrays with antibody to AXL revealed moderate-to-strong AXL protein expression with cytoplasmic and nuclear localization in clinically localized PCa samples (Figure 2*A*). AXL protein expression was enhanced with increasing tumor grade (Figure 2, *A* and *B*). In addition, the bone metastatic lesions showed intense AXL expression compared with lymph node metastatic lesions (Figure 2*C*). To further address the relationship between AXL and Anxa2 in PCa, tissue microarrays were analyzed by costaining with anti-AXL antibody and anti-Anxa2 antibody. Interestingly, the expression of AXL was inversely proportional to the expression of Anxa2 in the primary site (Figure 3). These data correlate to the previous observations that the loss of Anxa2 expression seems to be specific for PCa disease [28–33]. These data suggest that PCa express AXL on their surface and that AXL expression may reflect tumor aggressiveness.

The data presented thus far also suggest that Anxa2 regulates the expression of AXL in PCa *in vitro*. To determine whether Anxa2 regulates AXL expression in PCa cells *in vivo*, we took advantage of an osteogenic assay in which neonatal skeletal elements are transplanted subcutaneously into recipient mice to form bone *in vivo* (e.g., vertebral body or "vossicles") [34,35]. Here, vertebral bodies excised from *Anxa2*$^{+/+}$ or *Anxa2*$^{-/-}$ animals were seeded with human PCa cells (PC3) before vossicle implantation into immunodeficient animals (Figure 4*A*). After

1 month, the vossicles were dissected, and the expression of AXL by the implanted PC3 was evaluated by immunohistochemistry. Significantly more AXL expression by PC3 cells was observed when the cancer cells were implanted into vossicles that expressed Anxa2 (Figure 4, *B* and *C*). Real-time PCR examination of the native bones of these animals did not detect significant human ALU signals derived from the human PCa cells, suggesting that the PCa cells did not migrate away from the *Anxa2*$^{-/-}$ vossicles (data not presented). These data suggest that Anxa2 regulates the expression of AXL in PCa *in vivo* and is critical for PCa growth in bone.

Osteoblasts Express GAS6

GAS6 is one of the known ligands for the AXL family of RTKs. Because osteoblasts represent critical cells that participate in the establishment of the HSC niche and express Anxa2, we explored whether osteoblasts also express GAS6. Primary human osteoblasts and the

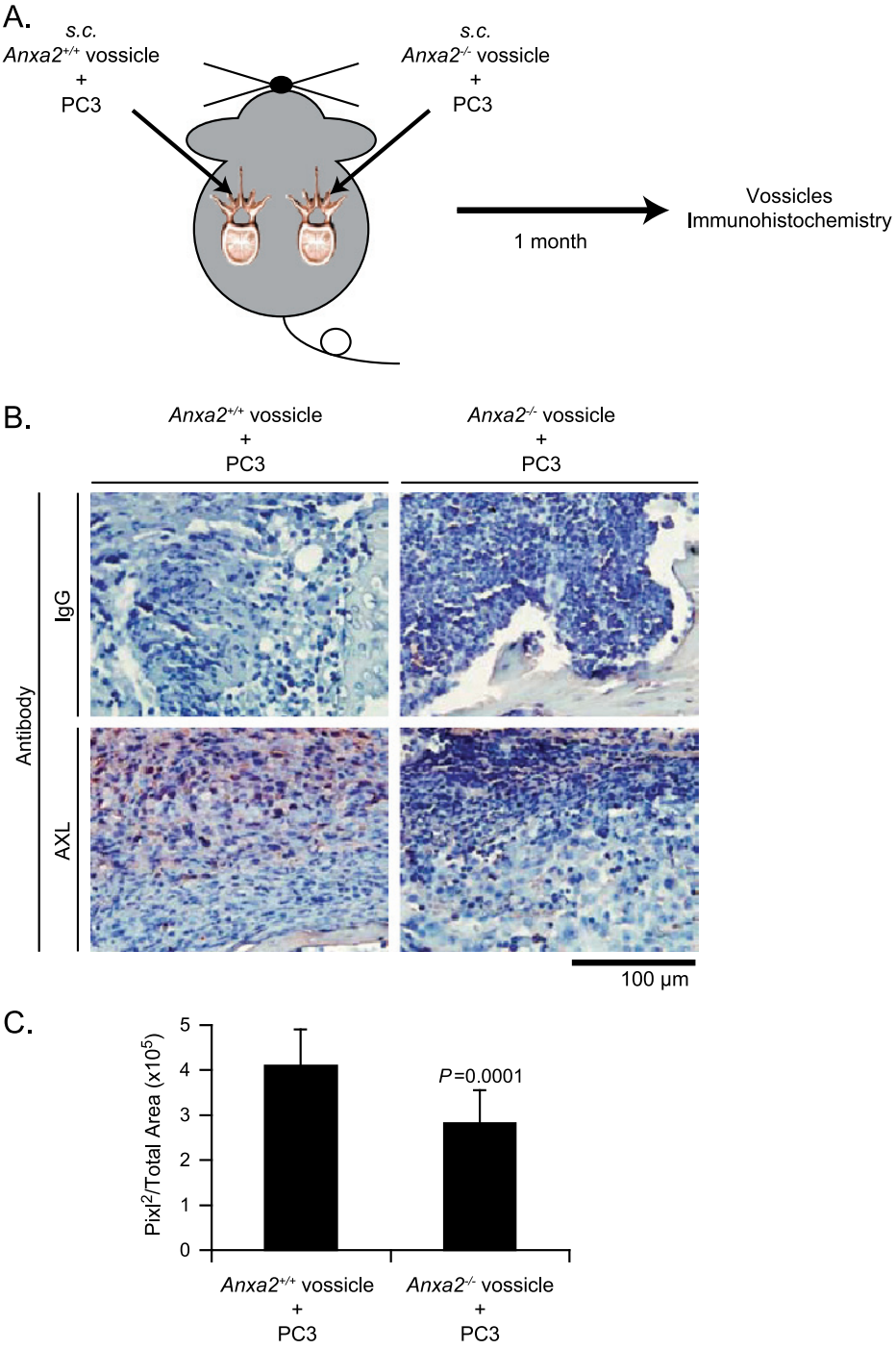

Figure 4. Anxa2-induced AXL expression of prostate cancer *in vivo*. (A) Experimental design. (B) PC3 cells (1×10^4 cells per 10 μl) were injected into vertebral bodies (vossicles) derived from *Anxa2*$^{+/+}$ and *Anxa2*$^{-/-}$ mice and transplanted into immunodeficient mice ($n = 12$). At 1 month after transplantation, the vossicles were dissected, and the AXL expression in the vossicles was evaluated by immunohistochemistry. Original magnification, ×60. Scale bar, 100 μm. (C) Quantitative analysis of AXL staining in (B). Data are presented as mean ± SD. *Significant difference from AXL staining of PCa grown in *Anxa2*$^{+/+}$ vossicles.

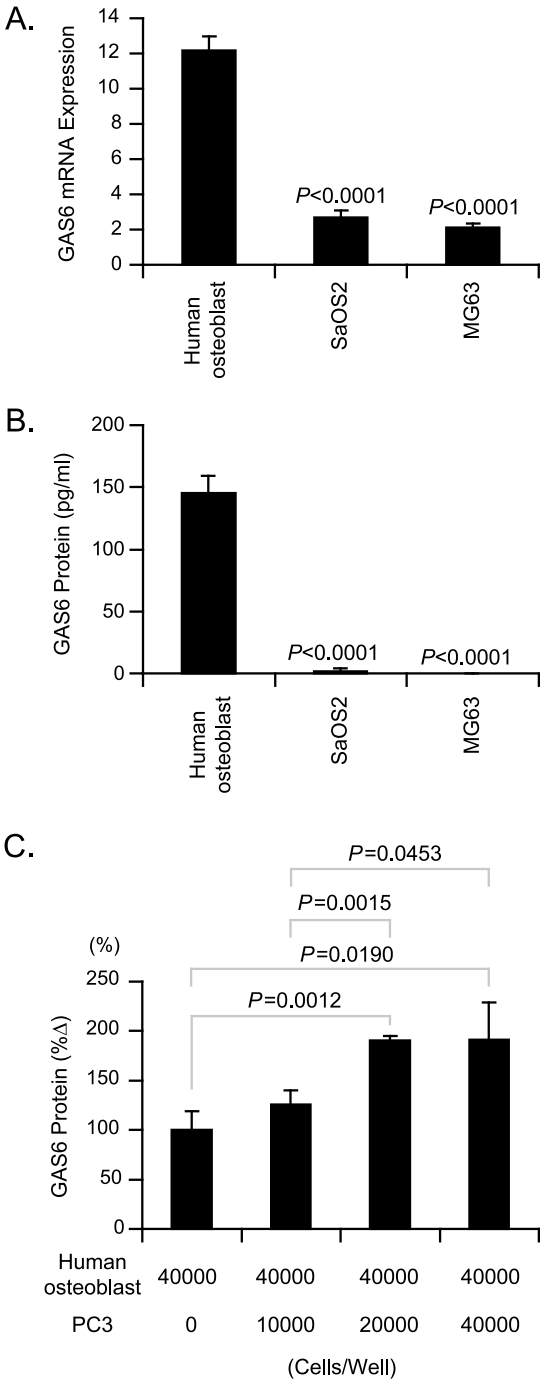

Figure 5. Osteoblasts express GAS6. (A) GAS6 mRNA levels in human osteoblasts and the osteosarcoma cell lines SaOS2 and MG63 were determined by real-time RT-PCR. Data were normalized to β-actin and presented as mean ± SD from three independent PCRs. *Significant differences from mRNA expressed by human osteoblasts. (B) Human osteoblasts, SaOS2, and MG63 (4×10^4 cells per well) were plated in 24-well plates in Dulbecco's modified Eagle medium (1 ml) without serum. (C) PC3 cells (0-4×10^4 cells) were seeded directly onto primary human osteoblast monolayers (4×10^4 cells) in 24-well tissue culture plates in serum-free conditions. At 48 hours, culture medium was collected. The levels of GAS6 were determined by ELISA, and supernatants were normalized by total protein concentration. Data are presented as mean ± SD from triplicate determinations. *Significant difference from human osteoblasts alone.

osteoblast-like human osteosarcoma cell lines SaOS2 and MG63 were evaluated by QRT-PCR for the expression of GAS6 mRNA. The data suggest that GAS6 mRNA was most strongly expressed by primary human osteoblasts (Figure 5*A*). To validate that GAS6 mRNA is translated into a mature secreted protein, GAS6 levels were evaluated in serum-free cell culture medium conditioned by primary human osteoblasts and human osteoblast-like cells. Primary human osteoblasts produced the most GAS6 in culture (145.6 ± 13.6 pg/ml) as detected by ELISA, followed by SaOS2 (1.5 ± 2.3 pg/ml) in a 48-hour period (Figure 5*B*). Next, to determine whether GAS6 synthesis occurs in response to PCa cells, cocultures of PC3 cells and the primary human osteoblasts were established, and cell culture–conditioned medium was collected after 48 hours. In the direct cell-to-cell contact cocultures, the productions of GAS6 were significantly stimulated compared with the primary human osteoblasts alone (Figure 5*C*). These data suggest that osteoblastic cells express GAS6, that human osteoblasts secrete GAS6, and that GAS6 synthesis occurs in response to PCa cells. Little to no GAS6, however, was identified in cell culture medium conditioned by the human osteosarcoma cell lines.

GAS6 Regulates the Invasion, Proliferation, Survival, and Cell Cycling of PCa

In many systems, the binding of GAS6 to AXL alters cellular functions including migration, proliferation, and survival [36–41]. We evaluated the effect of GAS6 on PCa in each of these cellular functions.

First, it was determined using *in vitro* invasion chambers that PCa cells migrate toward GAS6 (Figure 6*A*).

Next, proliferation assays demonstrated that GAS6 inhibited the proliferation of PC3 and DU145 cells in a dose-dependent manner (Figure 6*B*). To further address potential mechanisms, proliferation of PC3 in response to GAS6 and/or Anxa2 with/without U0126 (MEK 1/2 inhibitor) treatment was examined. As before, GAS6 inhibited the proliferation of PC3, whereas no further enhancements were observed in response to Anxa2 treatment (Figure 6*C*). In addition, when the cells were treated with Anxa2 and GAS6, the proliferation of PC3 cells was inhibited (Figure 6*C*). However, when the cells were pretreated with U0126, all of those effects were offset (Figure 6*C*).

The observation that GAS6 reduced PCa proliferation *in vitro* prompted our studies to determine whether GAS6 also protects PCa from apoptotic cell death. For these studies, PCa cells were extensively washed and then starved serum in the presence or absence of GAS6. After 24 hours, apoptotic cells were detected by flow cytometry using annexin V staining. The data demonstrate that fewer apoptotic cells were detected in GAS6-treated cells than controls (Figure 6*D*, *left*). To determine whether the reduced proliferation of PCa cells in response to GAS6 protects PCa cells from chemotherapy, the viability of PC3 cells subjected to chemotherapy was evaluated. PC3 cells were incubated with Taxotere in the presence or absence of GAS6. Annexin V staining was used to evaluate apoptosis induction. The inclusion of GAS6 in PCa cell cultures treated with Taxotere reduced the levels of annexin V staining compared with vehicle controls (Figure 6*D*, *right*). To further address the relationship between Anxa2 and GAS6 in the induction of PCa chemoresistance, PC3 cells were treated with Anxa2 and/or GAS6 before Taxotere treatment. Surprisingly, Anxa2 did not protect PC3 cells from chemotherapy, but when the PC3 cells were treated with Anxa2 and GAS6, the effects on protection of PC3 cells from chemotherapy were enhanced (Figure 6*E*).

Finally, to address whether GAS6 induces PCa into a dormant state, cell cycling states were evaluated by flow cytometry in the absence and

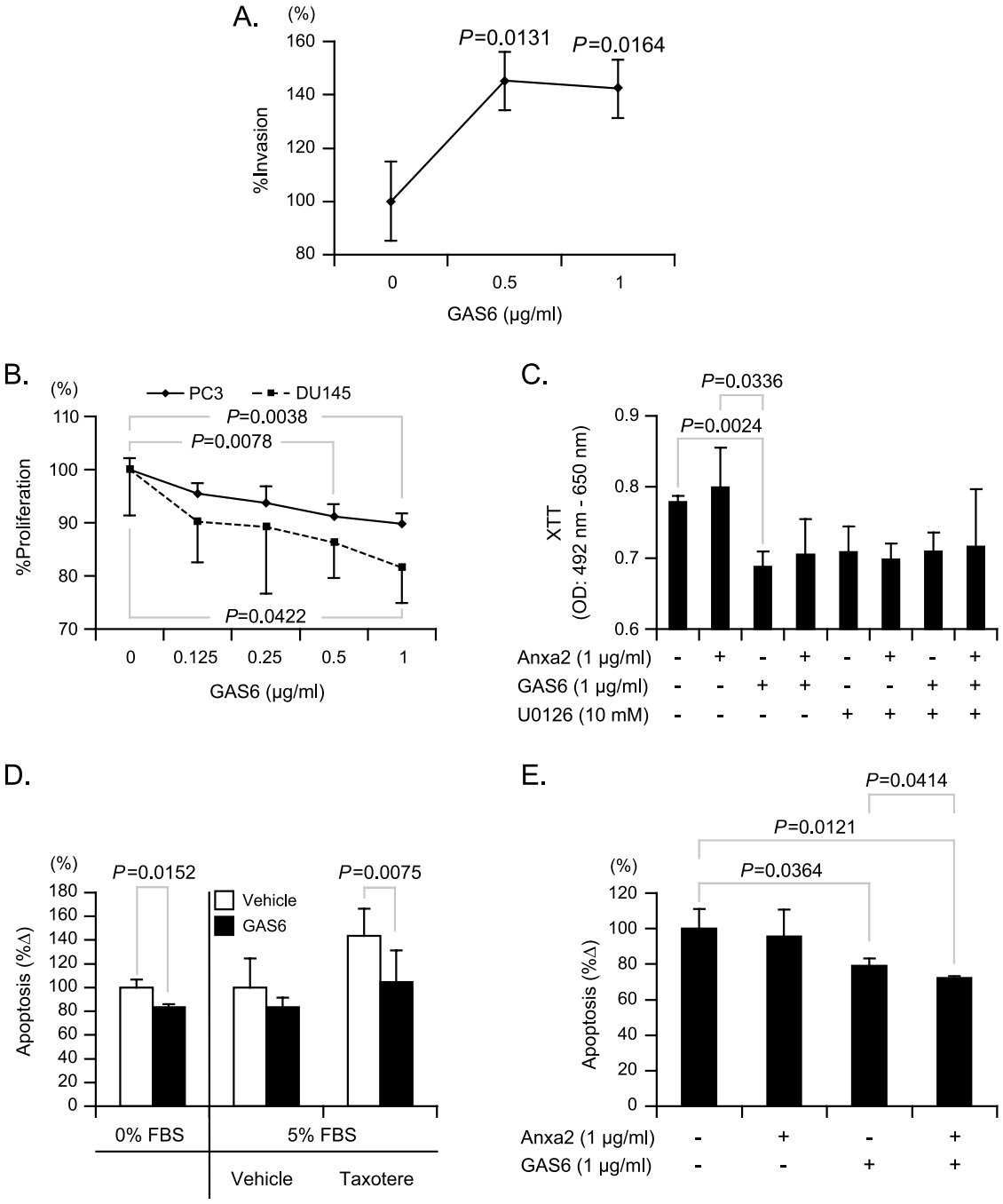

Figure 6. GAS6 regulates the invasion, proliferation, and apoptosis of PCa cell lines. (A) Matrigel invasion assays were performed to measure the treatment effect of GAS6 (0-1 μg/ml) on PC3 cell invasion. Data are presented as mean ± SD from triplicate determinations. *Significant different from spontaneous invasion. GAS6 inhibits cell proliferation in PCa cell lines (DU145 and PC3) in a dose-dependent manner. (B) DU145 and PC3 were seeded at 5000 cells per well in 96-well plates and were cultured with 0.1% FBS in the presence or absence of GAS6 (0-1 μg/ml). After 48 hours, cell proliferation was assessed using the XTT assay. Data are presented as mean ± SD from triplicate determinations. *Significant difference from vehicle treatment. (C) PC3 were seeded at 5000 cells per well in 96-well plates and were cultured with 0.1% FBS in the presence or absence of GAS6 (1 μg/ml) and/or Anxa2 (1 μg/ml). In some cases, the cells were pretreated with U0126 (10 μM) for 1 hour. After 48 hours, cell proliferation was assessed using XTT assay. Data are presented as mean ± SD from triplicate determinations. The effects of GAS6 on apoptosis and drug resistance of PCa were measured by annexin V staining. (D) Left: PC3 were treated with GAS6 (1 μg/ml) in serum-free medium for 24 hours. The percentage of apoptotic cells was assessed by flow cytometry. Right: PC3 were incubated with Taxotere after 24 hours with GAS6 (1 μg/ml) treatment in medium containing 5% FBS. Data are presented as mean ± SD from triplicate determinations. *Significant difference from vehicle treatment. (E) PC3 were incubated with Taxotere after 24 hours with GAS6 (1 μg/ml) and/or Anxa2 (1 μg/ml) treatment in medium containing 5% FBS. After 48 hours of incubation, the percentage of apoptotic cells was assessed by flow cytometry. Data are presented as mean ± SD from triplicate determinations.

Table 1. Effects of Anxa2 and GAS6 on the Cell Cycling State of PC3.

Cell Cycle	% Cell (*P* *vs* Vehicle Treatment)			
	Vehicle	Anxa2	GAS6	Anxa2 + GAS6
G_0	28.3 ± 0.7	33.0 ± 0.7 (*P* = .0011)	32.9 ± 0.7 (*P* = .0011)	32.0 ± 1.4 (*P* = .0151)
G_1	58.9 ± 0.2	56.5 ± 0.7 (*P* = .0036)	56.7 ± 0.3 (*P* = .0003)	57.4 ± 1.4 (*P* = .1487)
$S/M/G_2$	12.8 ± 0.5	10.5 ± 0.0 (*P* = .0014)	10.4 ± 0.4 (*P* = .0029)	10.6 ± 0.2 (*P* = .0024)

PC3 were treated with Anxa2 (1 μg/ml) and/or GAS6 (1 μg/ml) in serum-free medium for 48 hours. Cell cycling states of PC3 were assessed by flow cytometry. Data are presented as mean ± SD from triplicate determinations. Significantly different from vehicle treatment.

presence of GAS6 and/or Anxa2. GAS6 increased the fraction of cells in G_0 and decreased the fraction in the G_1 and $S/M/G_2$ states (Table 1). However, GAS6 and Anxa2 showed no synergic effects on cell cycling states (Table 1).

Taken together, these data suggest that GAS6 supports the PCa invasion, inhibits PCa proliferation through the MAPK signaling pathway, prevents apoptosis of PCa, protects PCa against chemotherapy, and regulates the cell cycling state of PCa. These data also suggest that the interaction of PCa with Anxa2 in the endosteal niche enhances their receptivity to GAS6, further suggesting a role for GAS6 in regulating the dormancy of PCa disseminating to the marrow.

Discussion

Several investigators have shown that the members of the AXL subfamily of RTKs—AXL, Sky, and Mer—are expressed in various types of cancers [40–49]. In result, it has been suggested that the AXL family RTKs may prove to be rationale targets for cancer therapy [49].

In this study, it was shown that the GAS6/AXL axis plays a role in regulating the invasion, proliferation, and survival of PCa. Initially, it was demonstrated that binding Anxa2 increases the expression of the AXL family of RTKs at an mRNA level, indicating a direct relationship between Anxa2/Anxa2r axis and the AXL subfamily of RTKs.

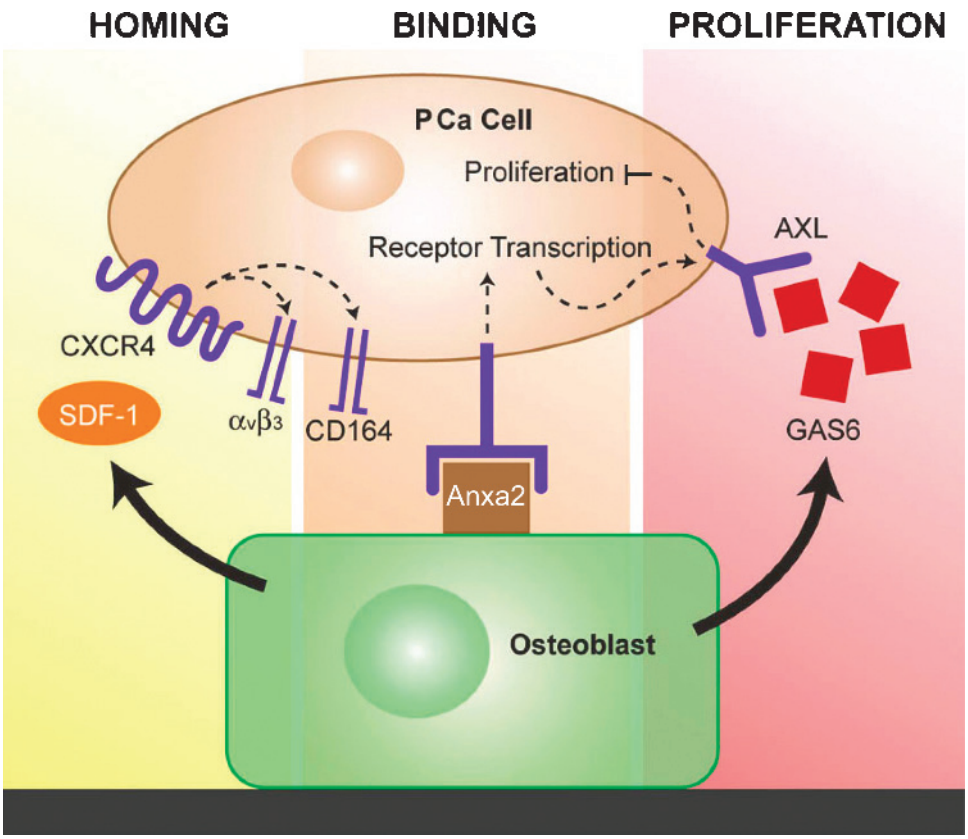

Figure 7. Dormancy of PCas is regulated by Anxa2 and GAS6 in the marrow. PCa cells display a remarkable ability to invade and survive in bone. The metastatic process is functionally similar to the migrational or "homing" behavior of hematopoietic cells to the bone marrow. Numerous molecules have been implicated in regulating HSC homing, participating as both chemoattractants and regulators of cell growth. Our previous work has demonstrated that PCa cells, like HSCs, use the CXC chemokine stromal–derived factor 1 (SDF-1 or CXCL12) and its receptor (CXCR4 or CXCR7/RDC1 [not shown]) to gain access to the bone marrow for metastasis formation and growth in bone. Engagement of SDF-1 receptors on PCa cells leads to increased expression of $\alpha_v\beta_3$ integrins, CD164, and Anxa2 that bind PCa to osteoblasts. Binding of PCa cells to Anxa2 induces transcription of the GAS6 family of receptors including AXL. AXL binding to GAS6 produced by osteoblasts induces quiescence of PCa cells and protects them from chemotherapy.

Subsequently, it was determined that the expression levels of AXL were significantly increased during metastasis to sites known to express high levels of Anxa2. We also demonstrated that GAS6 regulates invasion of PCa, inhibits PCa proliferation, protects PCa from chemotherapy, and alters the cell cycling state of PCa. It was also demonstrated that human osteoblasts express GAS6. Together, these data strongly suggest that the GAS6/AXL axis plays a regulatory role in the growth of PCa in the bone marrow. Furthermore, this regulation is achieved by 1) enhancing the PCa expression of the AXL family of RTKs when PCa cells bind to Anxa2 on osteoblasts and 2) secreting GAS6 as a paracrine signal by osteoblasts in the endosteal niche (see model, Figure 7).

In marrow, GAS6 is thought to be constitutively produced by fibroblasts and other stromal cells that support hematopoiesis [21,50]. It has been widely reported that GAS6 alters proliferation and survival of several different types of cancer cells [36–38,40,41]. The present study demonstrated that GAS6 inhibited the proliferation of PCa cells while protecting them from apoptotic cell death. However, these data are in conflict with those reported previously using similar cells. For example, the report by Sainaghi et al. [40] suggests that GAS6/AXL interactions are mitogenic for human PCa cell lines [51,52]. Moreover, the effect was proportional to AXL expression and not due to the inhibition of apoptosis [40]. Wu et al. [41] also reported that overexpression of the Mer occurs in a subset of PCa cells including the DU145 cell line. Here, too, activation of Mer did not result in increased proliferation. Rather, it stimulated the production of endocrine factors including chemokines such as IL-8 through transcriptional induction of the MEK/ERK/Jun/Fos pathway. It is unclear why our results differ from these previous reports. However, our results are in keeping with the concept that metastatic PCa parasitize the HSC niche [53]. Similarly, we have also shown that GAS6 supported survival, prevented apoptosis from chemotherapy, and regulated cell cycling in Mer-positive B-cell precursor acute lymphoblastic leukemia [54].

Our recent studies have shown that Anxa2, in addition to SDF-1, is produced by osteoblasts and plays an important role in the adhesion of HSCs to the endosteal niche [15,55]. The concept of "stem cell niche" has been proposed based on observations that HSCs are found in discrete areas in the bone marrow [56]. The stem cell niche is thought to regulate HSC self-renewal, proliferation, and differentiation through production of cytokines and cellular signals that are initiated by cell-to-cell adhesive interactions between HSCs and the components of the stem cell niche. Recent studies have demonstrated that osteoblasts comprise a crucial component of the HSC niche, "the endosteal niche," and cells of other lineage, including endothelial cells, probably participate in these stem cell functions. HSCs express the Anxa2r as well as CXCR4, which bind Anxa2 and SDF-1, respectively, and enable homing of HSCs to the endosteal niche. Similarly, PCa cells express both these molecules and seem to also use the same niche when homing to the bone marrow [9].

By-in-large, the role of the niche is thought to be the induction HSC dormancy. If metastatic PCa cells occupy a similar or the same ecological niche as HSCs themselves, then it is likely that the initial role of the HSC niche will be to induce dormancy in metastatic cells. In this study, GAS6 inhibited PCa proliferation, supported PCa survival, prevented PCa apoptosis from chemotherapy, and regulated cell cycling of PCa. Thus, these data suggest that GAS6/AXL axis is a potential target to metastasized PCa therapy. Previously, it was demonstrated that GAS6 expression by stromal cells reduces cell cycling of HSCs [21]. Our observations suggest a similar response by PCa. Although further study will clearly be needed, our results suggest that the activation of GAS6 receptors on PCa in the marrow environment may play a critical role as a molecular switch to establish dormancy.

Acknowledgments

The authors thank Amgen for providing recombinant human GAS6. The authors thank Laurie K. McCauley and Evan T. Keller for scientific discussions and Chris Jung for artwork. The authors also thank Katherine A. Hajjar (Weill Medical College of Cornell University, New York, NY) for the *Anxa2*$^{-/-}$ mice.

References

[1] Coleman RE (2006). Clinical features of metastatic bone disease and risk of skeletal morbidity. *Clin Cancer Res* **12**, 6243s–6249s.

[2] Taichman RS (2005). Blood and bone: two tissues whose fates are intertwined to create the hematopoietic stem-cell niche. *Blood* **105**, 2631–2639.

[3] Taichman RS and Emerson SG (1994). Human osteoblasts support hematopoiesis through the production of granulocyte colony-stimulating factor. *J Exp Med* **179**, 1677–1682.

[4] Arai F, Hirao A, Ohmura M, Sato H, Matsuoka S, Takubo K, Ito K, Koh GY, and Suda T (2004). Tie2/angiopoietin-1 signaling regulates hematopoietic stem cell quiescence in the bone marrow niche. *Cell* **118**, 149–161.

[5] Calvi LM, Adams GB, Weibrecht KW, Weber JM, Olson DP, Knight MC, Martin RP, Schipani E, Divieti P, Bringhurst FR, et al. (2003). Osteoblastic cells regulate the haematopoietic stem cell niche. *Nature* **425**, 841–846.

[6] Zhang J, Niu C, Ye L, Huang H, He X, Tong WG, Ross J, Haug J, Johnson T, Feng JQ, et al. (2003). Identification of the haematopoietic stem cell niche and control of the niche size. *Nature* **425**, 836–841.

[7] Kiel MJ, Yilmaz OH, Iwashita T, Terhorst C, and Morrison SJ (2005). SLAM family receptors distinguish hematopoietic stem and progenitor cells and reveal endothelial niches for stem cells. *Cell* **121**, 1109–1121.

[8] Taichman RS, Cooper C, Keller ET, Pienta KJ, Taichman NS, and McCauley LK (2002). Use of the stromal cell–derived factor-1/CXCR4 pathway in prostate cancer metastasis to bone. *Cancer Res* **62**, 1832–1837.

[9] Shiozawa Y, Havens AM, Jung Y, Ziegler AM, Pedersen EA, Wang J, Lu G, Roodman GD, Loberg RD, Pienta KJ, et al. (2008). Annexin II/annexin II receptor axis regulates adhesion, migration, homing, and growth of prostate cancer. *J Cell Biochem* **105**, 370–380.

[10] Pantel K, Alix-Panabieres C, and Riethdorf S (2009). Cancer micrometastases. *Nat Rev Clin Oncol* **6**, 339–351.

[11] Morgan TM, Lange PH, Porter MP, Lin DW, Ellis WJ, Gallaher IS, and Vessella RL (2009). Disseminated tumor cells in prostate cancer patients after radical prostatectomy and without evidence of disease predicts biochemical recurrence. *Clin Cancer Res* **15**, 677–683.

[12] Nash KT, Phadke PA, Navenot JM, Hurst DR, Accavitti-Loper MA, Sztul E, Vaidya KS, Frost AR, Kappes JC, Peiper SC, et al. (2007). Requirement of KISS1 secretion for multiple organ metastasis suppression and maintenance of tumor dormancy. *J Natl Cancer Inst* **99**, 309–321.

[13] Miura Y, Gao Z, Miura M, Seo BM, Sonoyama W, Chen W, Gronthos S, Zhang L, and Shi S (2006). Mesenchymal stem cell–organized bone marrow elements: an alternative hematopoietic progenitor resource. *Stem Cells* **24**, 2428–2436.

[14] Raynal P and Pollard HB (1994). Annexins: the problem of assessing the biological role for a gene family of multifunctional calcium- and phospholipid-binding proteins. *Biochim Biophys Acta* **1197**, 63–93.

[15] Jung Y, Wang J, Song J, Shiozawa Y, Havens A, Wang Z, Sun YX, Emerson SG, Krebsbach PH, and Taichman RS (2007). Annexin II expressed by osteoblasts and endothelial cells regulates stem cell adhesion, homing, and engraftment following transplantation. *Blood* **110**, 82–90.

[16] Hafizi S and Dahlback B (2006). Signalling and functional diversity within the Axl subfamily of receptor tyrosine kinases. *Cytokine Growth Factor Rev* **17**, 295–304.

[17] Neubauer A, Fiebeler A, Graham DK, O'Bryan JP, Schmidt CA, Barckow P, Serke S, Siegert W, Snodgrass HR, Huhn D, et al. (1994). Expression of axl, a transforming receptor tyrosine kinase, in normal and malignant hematopoiesis. *Blood* **84**, 1931–1941.

[18] Crosier PS, Hall LR, Vitas MR, Lewis PM, and Crosier KE (1995). Identification of a novel receptor tyrosine kinase expressed in acute myeloid leukemic blasts. *Leuk Lymphoma* **18**, 443–449.

[19] Avanzi GC, Gallicchio M, Cavalloni G, Gammaitoni L, Leone F, Rosina A, Boldorini R, Monga G, Pegoraro L, Varnum B, et al. (1997). GAS6, the ligand

of Axl and Rse receptors, is expressed in hematopoietic tissue but lacks mitogenic activity. *Exp Hematol* **25**, 1219–1226.

[20] Satomura K, Derubeis AR, Fedarko NS, Ibaraki-O'Connor K, Kuznetsov SA, Rowe DW, Young MF, and Gehron Robey P (1998). Receptor tyrosine kinase expression in human bone marrow stromal cells. *J Cell Physiol* **177**, 426–438.

[21] Dormady SP, Zhang XM, and Basch RS (2000). Hematopoietic progenitor cells grow on 3T3 fibroblast monolayers that overexpress growth arrest–specific gene-6 (GAS6). *Proc Natl Acad Sci USA* **97**, 12260–12265.

[22] Jiang HY, Lee KH, Schneider C, O WS, Tang PL, and Chow PH (2001). The growth arrest specific gene (gas6) protein is expressed in abnormal embryos sired by male golden hamsters with accessory sex glands removed. *Anat Embryol (Berl)* **203**, 343–355.

[23] Wu TT, Sikes RA, Cui Q, Thalmann GN, Kao C, Murphy CF, Yang H, Zhau HE, Balian G, and Chung LW (1998). Establishing human prostate cancer cell xenografts in bone: induction of osteoblastic reaction by prostate-specific antigen-producing tumors in athymic and SCID/bg mice using LNCaP and lineage-derived metastatic sublines. *Int J Cancer* **77**, 887–894.

[24] Sun YX, Fang M, Wang J, Cooper CR, Pienta KJ, and Taichman RS (2007). Expression and activation of $\alpha_v\beta_3$ integrins by SDF-1/CXC12 increases the aggressiveness of prostate cancer cells. *Prostate* **67**, 61–73.

[25] Wang J, Shiozawa Y, Wang Y, Jung Y, Pienta KJ, Mehra R, Loberg R, and Taichman RS (2008). The role of CXCR7/RDC1 as a chemokine receptor for CXCL12/SDF-1 in prostate cancer. *J Biol Chem* **283**, 4283–4294.

[26] Gothot A, Pyatt R, McMahel J, Rice S, and Srour EF (1997). Functional heterogeneity of human CD34(+) cells isolated in subcompartments of the G_0/G_1 phase of the cell cycle. *Blood* **90**, 4384–4393.

[27] Fridell YW, Jin Y, Quilliam LA, Burchert A, McCloskey P, Spizz G, Varnum B, Der C, and Liu ET (1996). Differential activation of the Ras/extracellular-signal–regulated protein kinase pathway is responsible for the biological consequences induced by the Axl receptor tyrosine kinase. *Mol Cell Biol* **16**, 135–145.

[28] Chetcuti A, Margan SH, Russell P, Mann S, Millar DS, Clark SJ, Rogers J, Handelsman DJ, and Dong Q (2001). Loss of annexin II heavy and light chains in prostate cancer and its precursors. *Cancer Res* **61**, 6331–6334.

[29] Banerjee AG, Liu J, Yuan Y, Gopalakrishnan VK, Johansson SL, Dinda AK, Gupta NP, Trevino L, and Vishwanatha JK (2003). Expression of biomarkers modulating prostate cancer angiogenesis: differential expression of annexin II in prostate carcinomas from India and USA. *Mol Cancer* **2**, 34.

[30] Kirshner J, Chen CJ, Liu P, Huang J, and Shively JE (2003). CEACAM1-4S, a cell-cell adhesion molecule, mediates apoptosis and reverts mammary carcinoma cells to a normal morphogenic phenotype in a 3D culture. *Proc Natl Acad Sci USA* **100**, 521–526.

[31] Liu JW, Shen JJ, Tanzillo-Swarts A, Bhatia B, Maldonado CM, Person MD, Lau SS, and Tang DG (2003). Annexin II expression is reduced or lost in prostate cancer cells and its re-expression inhibits prostate cancer cell migration. *Oncogene* **22**, 1475–1485.

[32] Smitherman AB, Mohler JL, Maygarden SJ, and Ornstein DK (2004). Expression of annexin I, II and VII proteins in androgen stimulated and recurrent prostate cancer. *J Urol* **171**, 916–920.

[33] Semov A, Moreno MJ, Onichtchenko A, Abulrob A, Ball M, Ekiel I, Pietrzynski G, Stanimirovic D, and Alakhov V (2005). Metastasis-associated protein S100A4 induces angiogenesis through interaction with annexin II and accelerated plasmin formation. *J Biol Chem* **280**, 20833–20841.

[34] Koh AJ, Demiralp B, Neiva KG, Hooten J, Nohutcu RM, Shim H, Datta NS, Taichman RS, and McCauley LK (2005). Cells of the osteoclast lineage as mediators of the anabolic actions of parathyroid hormone in bone. *Endocrinology* **146**, 4584–4596.

[35] Pettway GJ and McCauley LK (2008). Ossicle and vossicle implant model systems. *Methods Mol Biol* **455**, 101–110.

[36] Holland SJ, Powell MJ, Franci C, Chan EW, Friera AM, Atchison RE, McLaughlin J, Swift SE, Pali ES, Yam G, et al. (2005). Multiple roles for the receptor tyrosine kinase axl in tumor formation. *Cancer Res* **65**, 9294–9303.

[37] Budagian V, Bulanova E, Orinska Z, Duitman E, Brandt K, Ludwig A, Hartmann D, Lemke G, Saftig P, and Bulfone-Paus S (2005). Soluble Axl is generated by ADAM10-dependent cleavage and associates with Gas6 in mouse serum. *Mol Cell Biol* **25**, 9324–9339.

[38] van Ginkel PR, Gee RL, Shearer RL, Subramanian L, Walker TM, Albert DM, Meisner LF, Varnum BC, and Polans AS (2004). Expression of the receptor tyrosine kinase Axl promotes ocular melanoma cell survival. *Cancer Res* **64**, 128–134.

[39] Son BK, Kozaki K, Iijima K, Eto M, Nakano T, Akishita M, and Ouchi Y (2007). Gas6/Axl-PI3K/Akt pathway plays a central role in the effect of statins on inorganic phosphate–induced calcification of vascular smooth muscle cells. *Eur J Pharmacol* **556**, 1–8.

[40] Sainaghi PP, Castello L, Bergamasco L, Galletti M, Bellosta P, and Avanzi GC (2005). Gas6 induces proliferation in prostate carcinoma cell lines expressing the Axl receptor. *J Cell Physiol* **204**, 36–44.

[41] Wu YM, Robinson DR, and Kung HJ (2004). Signal pathways in up-regulation of chemokines by tyrosine kinase MER/NYK in prostate cancer cells. *Cancer Res* **64**, 7311–7320.

[42] O'Bryan JP, Frye RA, Cogswell PC, Neubauer A, Kitch B, Prokop C, Espinosa R III, Le Beau MM, Earp HS, and Liu ET (1991). *axl*, a transforming gene isolated from primary human myeloid leukemia cells, encodes a novel receptor tyrosine kinase. *Mol Cell Biol* **11**, 5016–5031.

[43] Rochlitz C, Lohri A, Bacchi M, Schmidt M, Nagel S, Fopp M, Fey MF, Herrmann R, and Neubauer A (1999). Axl expression is associated with adverse prognosis and with expression of Bcl-2 and CD34 in *de novo* acute myeloid leukemia (AML): results from a multicenter trial of the Swiss Group for Clinical Cancer Research (SAKK). *Leukemia* **13**, 1352–1358.

[44] Wimmel A, Glitz D, Kraus A, Roeder J, and Schuermann M (2001). Axl receptor tyrosine kinase expression in human lung cancer cell lines correlates with cellular adhesion. *Eur J Cancer* **37**, 2264–2274.

[45] Shieh YS, Lai CY, Kao YR, Shiah SG, Chu YW, Lee HS, and Wu CW (2005). Expression of *axl* in lung adenocarcinoma and correlation with tumor progression. *Neoplasia* **7**, 1058–1064.

[46] Chung BI, Malkowicz SB, Nguyen TB, Libertino JA, and McGarvey TW (2003). Expression of the proto-oncogene *Axl* in renal cell carcinoma. *DNA Cell Biol* **22**, 533–540.

[47] Meric F, Lee WP, Sahin A, Zhang H, Kung HJ, and Hung MC (2002). Expression profile of tyrosine kinases in breast cancer. *Clin Cancer Res* **8**, 361–367.

[48] Wu CW, Li AF, Chi CW, Lai CH, Huang CL, Lo SS, Lui WY, and Lin WC (2002). Clinical significance of AXL kinase family in gastric cancer. *Anticancer Res* **22**, 1071–1078.

[49] Zhang YX, Knyazev PG, Cheburkin YV, Sharma K, Knyazev YP, Orfi L, Szabadkai I, Daub H, Keri G, and Ullrich A (2008). AXL is a potential target for therapeutic intervention in breast cancer progression. *Cancer Res* **68**, 1905–1915.

[50] Manfioletti G, Brancolini C, Avanzi G, and Schneider C (1993). The protein encoded by a growth arrest–specific gene (*gas6*) is a new member of the vitamin K–dependent proteins related to protein S, a negative coregulator in the blood coagulation cascade. *Mol Cell Biol* **13**, 4976–4985.

[51] Robinson D, He F, Pretlow T, and Kung HJ (1996). A tyrosine kinase profile of prostate carcinoma. *Proc Natl Acad Sci USA* **93**, 5958–5962.

[52] Jacob AN, Kalapurakal J, Davidson WR, Kandpal G, Dunson N, Prashar Y, and Kandpal RP (1999). A receptor tyrosine kinase, UFO/Axl, and other genes isolated by a modified differential display PCR are overexpressed in metastatic prostatic carcinoma cell line DU145. *Cancer Detect Prev* **23**, 325–332.

[53] Shiozawa Y, Havens AM, Pienta KJ, and Taichman RS (2008). The bone marrow niche: habitat to hematopoietic and mesenchymal stem cells, and unwitting host to molecular parasites. *Leukemia* **22**, 941–950.

[54] Shiozawa Y, Pedersen EA, and Taichman RS (in press). GAS6/Mer axis regulates the homing and survival of the E2A/PBX1–positive B-cell precursor acute lymphoblastic leukemia in the bone marrow niche. *Exp Hematol.*

[55] Jung Y, Wang J, Schneider A, Sun YX, Koh-Paige AJ, Osman NI, McCauley LK, and Taichman RS (2006). Regulation of SDF-1 (CXCL12) production by osteoblasts; a possible mechanism for stem cell homing. *Bone* **38**, 497–508.

[56] Schofield R (1978). The relationship between the spleen colony–forming cell and the haemopoietic stem cell. *Blood Cells* **4**, 7–25.

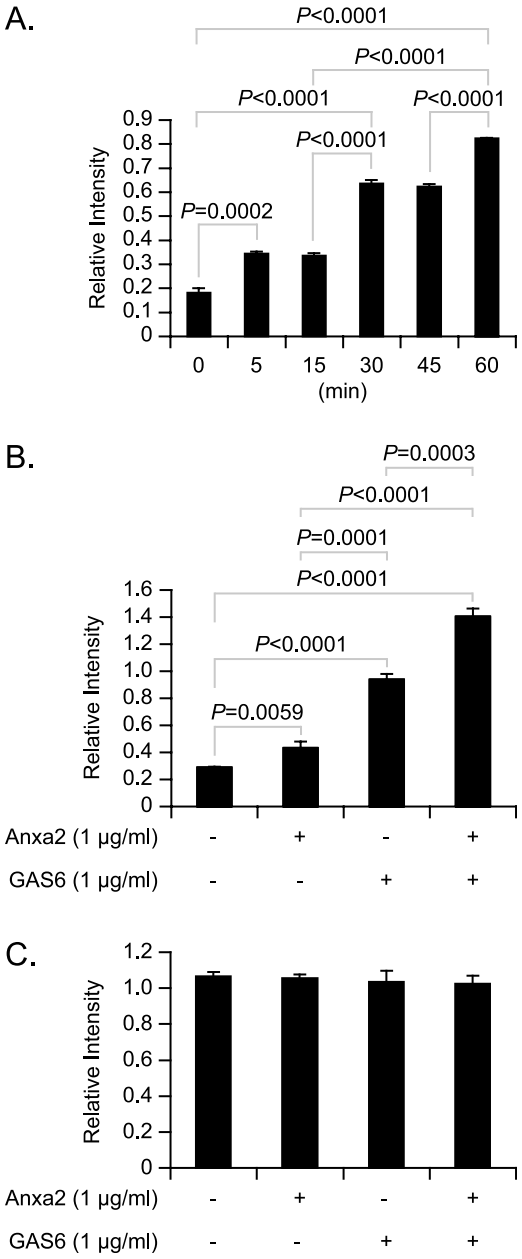

Figure W1. Quantitative analysis of Western blots. The densities of the Western blot bands were quantified with ImageJ software. (A) Quantitative analysis of phosphorylated Erk1/2 in PC3 cells that were treated with GAS6 in Figure 1*D*. (B) Quantitative analysis of phosphorylated Erk1/2 in PC3 cells that were treated with Anxa2 and/or GAS6 in Figure 1*E*. (C) Quantitative analysis of phosphorylated Erk1/2 in SaOS2 cells that were treated with Anxa2 and/or GAS6 in Figure 1*E*. Data are presented as mean ± SD from triplicate determinations.